Elsevier Editorial System(tm) for Membrane Science
Manuscript Draft

Manuscript Number:

Title: Influence of membrane thickness and process conditions on Direct Contact Membrane Distillation at different salinities.

Article Type: Full Length Article

Keywords: Brine treatment , Crystallization, DCMD, Energy Efficiency, Optimal thickness

Corresponding Author: Ms. Lies Eykens,

Corresponding Author's Institution: VITO NV

First Author: Lies Eykens

Order of Authors: Lies Eykens; Ivaylo Hitsov; Kristien De Sitter; Chris Dotremont; Luc Pinoy; Ingmar Nopens; Bart Van der Bruggen

Abstract: Membrane distillation is an emerging thermal membrane technology for the separation of salts and other non-volatile inclusions from water streams. The process offers a solution for the treatment of concentrated solutions, which are out of the scope of reverse osmosis. However, only few studies focused on the optimal membrane properties and operational conditions in the high concentration regime. In this paper, membranes with variations in thickness, porosity and structure are experimentally investigated in direct contact membrane distillation (DCMD) as well as simulated, using the Dusty Gas Model. Operational conditions, including the temperature difference over the membrane, the flow velocity and the feed stream salinity up to saturation are varied. It is confirmed that for pure water, thinner membranes show higher fluxes, while energy efficiency is unaffected by membrane thickness. At higher salinities, an optimal membrane thickness depending on membrane parameters and process conditions exists. The optimal membrane thickness is calculated in this article for concentrations of NaCl ranging from 0 up to 320 g/l and variations in bulk temperature difference and flow velocities for four different membranes.

Suggested Reviewers: Hendrik Müller-Holst
Memsys clearwater Pte. Ltd.
hendrik.mueller-holst@memsys.eu

Corinne Cabassud
Professor, Biosystems and Process Engineering Laboratory, Institut National des Sciences Appliquées de Toulouse
corinne.cabassud@insa-toulouse.fr

Cejna Anna Quist-Jensen
ITM-CNR
cejnaquist@gmail.com

Cover Letter

Click here to download Cover Letter: Cover Letter.docx

Lies Eykens

VITO NV – Flemish institute for technological research

PhD Student

Boeretang 200

2480 Mol, Belgium

Email: lies.eykens@vito.be

Dear Sir/Madam,

Please find attached the electronic file of our paper entitled “Influence of membrane thickness and process conditions on Direct Contact Membrane Distillation at different salinities” for possible publication in Journal of Membrane Science.

In this paper, membranes with thickness ranging from 20 - 188 µm, variations in porosity and different structure are experimentally investigated and simulated using the Dusty Gas Model. Multiple process conditions are used for exploring the entire solubility range of NaCl. In addition, the optimal membrane thickness is computed, depending on process conditions and membrane structure. Furthermore, guidelines are proposed for the choice of membrane and operational conditions to optimize the DCMD process.

All the authors mutually agree on submitting our manuscript to Journal of Membrane Science and the manuscript is an original work of the authors. Moreover, none of the work described in this manuscript has been submitted earlier to Journal of Membrane Science. The manuscript consists of 23 pages; include 4 tables and 10 figures.

Sincerely,

Lies Eykens

26-02-2014.

HIGHLIGHTS

- The DCMD performance of different membranes was evaluated
- The whole solubility range of NaCl was investigated
- Effect of salinity on flux and energy efficiency was studied
- Guidelines are given for choice of membrane and operational conditions
- Calculation of optimal membrane thickness was performed

INFLUENCE OF MEMBRANE THICKNESS AND PROCESS CONDITIONS ON DIRECT CONTACT MEMBRANE DISTILLATION AT DIFFERENT SALINITIES

L. Eykens[1,2*], I. Hitsov[1,3*], K. De Sitter[1], C. Dotremont[1], L. Pinoy[4], I. Nopens[3], B. Van der Bruggen[2]

[1]VITO - Flemish Institute for Technological Research, Boeretang 200, 2400 Mol, Belgium

[2]Department of Chemical Engineering, Process Engineering for Sustainable Systems Section, KU Leuven, W. de Croylaan 46, 3001 Leuven, Belgium

[3]BIOMATH, Department of Mathematical Modelling, Statistics and Bioinformatics, Faculty of Bioscience Engineering, Ghent University, Coupure Links 653, 9000 Ghent, Belgium

[4]Department of Chemical Engineering, Cluster Sustainable Chemical Process Technology, KU Leuven, Gebroeders Desmetstraat 1, Ghent B-9000, Belgium

*Email: lies.eykens@vito.be, ivaylo.hitsov@vito.be

Abstract

Membrane distillation is an emerging thermal membrane technology for the separation of salts and other non-volatile inclusions from water streams. The process offers a solution for the treatment of concentrated solutions, which are out of the scope of reverse osmosis. However, only few studies focused on the optimal membrane properties and operational conditions in the high concentration regime. In this paper, membranes with variations in thickness, porosity and structure are experimentally investigated in direct contact membrane distillation (DCMD) as well as simulated, using the Dusty Gas Model. Operational conditions, including the temperature difference over the membrane, the flow velocity and the feed stream salinity up to saturation are varied. It is confirmed that for pure water, thinner membranes show higher fluxes, while energy efficiency is unaffected by membrane thickness. At higher salinities, an optimal membrane thickness depending on membrane parameters and process conditions exists. The optimal membrane thickness is calculated in this article for concentrations of NaCl ranging from 0 up to 320 g/l and variations in bulk temperature difference and flow velocities for four different membranes.

Keywords: Brine treatment , Crystallization, DCMD, Energy Efficiency, Optimal thickness

NOMENCLATURE

a	Activity	-
B	Permeability	$\mathrm{kg/(m^2.h.Pa)}$
C_p	Heat capacity	$\mathrm{J/(kg.K)}$
D	Diffusion coefficient	$\mathrm{m^2/s}$
d	Pore diameter	m
DCMD	Direct Contact Membrane Distillation	-
EE	Energy efficiency	%
F	Mass flow rate in the channels	$\mathrm{kg/s}$
GLUE	Generalized Likelihood Uncertainty Estimation	-
k_m	Membrane thermal conductivity	$\mathrm{W/(m.K)}$
LEP	Liquid entry pressure	Pa
M	Molar mass	$\mathrm{kg/mol}$
m	Molality	$\mathrm{mol/kg}$
N	Flux	$\mathrm{kg/(m^2.h)}$
P	Pressure	Pa
PES	Polyethersulfone	-
PP	Polypropylene	-
PTFE	Polytetrafluoroethylene	-
PVDF	Polyvinylidene fluoride	-
Q	Heat flux through the membrane	$\mathrm{W/m^2}$
r	Pore radius	m
R	Universal gas constant	$\mathrm{J/(kg.mol)}$
SEM	Scanning electron microscopy	-
T	Temperature	K
V	Volume	L
v	Flow velocity in the channels	$\mathrm{m/s}$
δ	Membrane thickness	m
ΔH	Enthalpy of vaporization	J/kg
Δp	Vapor pressure difference over the membrane	bar

ΔT	Temperature difference over the membrane	K
ε	Porosity	%
τ	Tortuosity	%

Subscripts

0	Pure water
Av	Average
b	Bulk
C	Conduction
f	Feed
i	Interfacial
In	Inlet
m	Membrane
Max	Maximum
N	Flux
Out	Outlet
p	Permeate
Po	Polymer
w	Water

1 INTRODUCTION

Membrane distillation is an emerging thermal membrane process, mainly aimed at desalination [1]. For seawater desalination, reverse osmosis is still more efficient compared to membrane distillation. Therefore, membrane distillation research is shifting from seawater desalination towards treatment of more concentrated solutions like brines, waste streams and recuperation of valuable components in the chemical, pharmaceutical and food industry [3]–[5]. These streams are out of the scope of reverse osmosis [2] and often membrane distillation is applied in combination with a crystallization step [5]–[7]. Research on treatment of these concentrates with membrane distillation focuses mainly on feasibility of the technique, prevention of scaling and control of the crystal formation [8]–[10]. While many studies regarding direct contact membrane distillation (DCMD) considered the optimal membrane properties for seawater desalination [4], [11]–[17] only few studies focused on the optimal membrane properties in the high concentration regime; mainly aiming at optimizing the membrane thickness. Gostoli et al. stated already in 1987 that for thin membranes the flux is more affected by concentration [18]. Other studies on the effect of thickness concluded that the optimal membrane thickness ranges from 10 to 60 µm, depending on concentration, heat transfer coefficients of the feed and permeate channels, feed inlet temperature and membrane permeability [19]–[21]. Furthermore, increasing the membrane thickness resulted in an improved energy efficiency up to asymptotic values depending on concentration and process conditions [19], [22]. A more detailed overview of the literature on membrane thickness is presented in Table 1. In a recently published review, Curcio and Drioli stated that the literature still lacks clear and conclusive statements concerning the thickness effect [23]. Additionally, only very few studies reported on the influence of operational conditions at high salinity [9], [24]–[26]. Therefore, in this paper, membranes with thickness ranging from 20 - 188 µm, variations in porosity and different structure are experimentally investigated and simulated in the entire solubility range of NaCl, varying the temperature difference over the membrane and the flow velocity. In addition, the optimal membrane thickness is computed as well as the effect of process conditions and membrane parameters on flux, energy efficiency and the optimal membrane thickness. From this investigation, guidelines are proposed for the choice of membrane and operational conditions to optimize the DCMD process in terms of flux and energy efficiency at high

concentrations.

Table 1: Overview of the literature regarding the effect of membrane thickness for saline streams

	Author	Membrane	Statement	[NaCl]	Conditions
Flux	Gostoli [18]	PTFE (60 µm) PTFE + air gap (1 cm)	Flux of thin membranes is more affected by salinity	0-30 g/kg	T_m = 50 °C ΔT= 5-30 °C v = 0.35 m/s
	Lagana [20]	PP, ENKA MD-020-2N-CP (120 µm)	Optimal δ (30 - 60 um)	Conditions not specified	
	Martinez [19]	GVHP (100 µm)	Optimal δ depending on concentration (10 - 60 um)	0-250 g/kg	T_f = 40 °C T_p= 20 °C v = 0.35 m/s
	Wu [21]	Electrospun PVDF (27 - 58 µm)	Optimal δ depending on heat transfer in the channels, feed temperature and membrane permeability (10 - 30 um)	0-100 g/kg	T_f = 45-65 °C T_p= 20 °C v = not specified
Energy efficiency	Martinez [19]	GVHP (100 µm), TF200 (60 µm)	Asymptotic value for larger δ, sharp decline of energy efficiency at low δ, especially at higher concentrations	0-250 g/kg	T_f = 40 °C T_p= 20 °C v = 0.35 m/s
	Essahli [22]	Electrospun PVDF (144 – 1529 µm)	Increase of δ results in an improved energy efficiency up to assymptotic values depending on process conditions	0-60 g/kg	T_f = 40-80 °C T_p= 20 °C v = not specified

2 THEORETICAL BACKGROUND

In membrane distillation, both flux and energy efficiency need to be optimized simultaneously. Both are influenced by process conditions, membrane structure and the temperature polarization, as schematized in Figure 1. The complex interplay between all these parameters makes modeling a very important part of membrane distillation research. The effect of the different parameters on membrane distillation performance is described in more detail in the next paragraphs. This theoretical background is limited to the important effects needed to explain the experimental results obtained in this study. More detailed reviews on this topic can be found elsewhere [1], [4], [23], [27], [28].

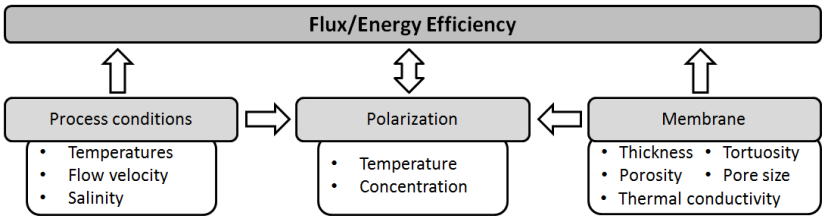

Figure 1: Parameters affecting the membrane distillation flux and energy efficiency

2.1 Factors affecting flux

The transmembrane flux N is proportional to the interfacial water vapor pressure difference Δp_i:

$$N = B * \Delta p_i, \quad (1)$$

where B is the membrane permeability.

2.1.1 Permeability

The membrane permeability depends both on the membrane characteristics and the governing transport mechanism. In DCMD, pore size ranges from 0.1 to 1 µm and transitional diffusion, governed by both Knudsen and molecular diffusion is assumed [28], [29]. It is generally accepted that the permeability is improved by reducing membrane thickness δ and tortuosity τ or by increasing porosity ε and pore size r [23], [30], [31].

2.1.2 Driving force

The vapor pressure for pure water p_0 in Pa can be calculated using Antoine's equation:

$$p_0 = e^{23.238-\frac{3841}{(T-45)}} \quad (2)$$

With T the corresponding temperature in Kelvin [32].

The actual vapor pressure is calculated based on interfacial temperatures of feed ($T_{f,i}$) and permeate ($T_{p,i}$), which differ from the measured bulk temperatures of feed ($T_{f,b}$) and permeate ($T_{p,b}$) due to temperature polarization. This results in a lower real interfacial temperature difference (ΔT_i) compared to the bulk temperature difference (ΔT_b). In general, temperature polarization is more pronounced for membranes that are more permeable, thinner or possessing a high thermal conductivity [33],[34]. Temperature polarization is also affected by the hydrodynamics, i.e., flow velocity, module design and fluid properties [35], [36]. The actual feed vapor pressure is influenced by the activity of water a_w, depending on the interfacial molality m of the feed. For NaCl solutions, the following equations are used for

the calculation of the interfacial vapor pressure difference [37]:

$$p = a_w p_0 \quad (3)$$

$$a_w = 1 - 0.03112m - 0.001482m^2 \quad (4)$$

$$\Delta p_i = p_{f,i} - p_{p,i} = a_w p_{0,f,i} - p_{p,i} \quad (5)$$

Figure 2 visualizes the effect of salinity on vapor pressure at different ΔT_i. The theoretical vapor pressure differences over the membrane are shown as a function of ΔT_i over the membrane at a constant average temperature of 52.5 °C for 0 and 300 g/kg. For pure water, Δp_i is positive. For 300 g/kg, for ΔT_i between 0 - 5 °C, Δp_i is negative. The feed vapor pressure reduction due to salinity induces an "osmotic" driving force from the feed with high salinity to the pure permeate, resulting in osmotic distillation [38]. Therefore, a minimum ΔT_i over the membrane – 5 °C in this specific case - is needed to avoid negative fluxes.

The vapor pressure reduction, seen as black line on Fig. 2, represents the relative effect of salts on Δp_i, hence on the flux and is much more pronounced at lower thermal driving force. It is defined as:

$$Reduction, \% = 100 \frac{\Delta \mathrm{pi}_0 - \Delta \mathrm{pi}_{[\mathrm{NaCl}]}}{\Delta \mathrm{pi}_0}$$

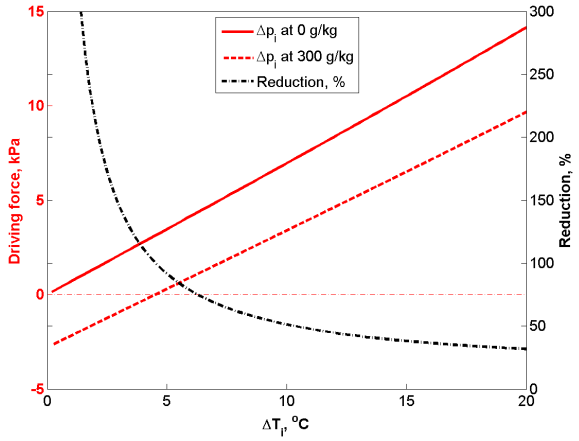

Figure 2: Driving force Δp_i calculated for pure water and 300 g/kg NaCl with equations 3 - 5 and the reduction of Δp_i in % due to salt as function of ΔT_i for T_{av} = 52.5 °C.

2.2 Factors affecting energy efficiency

Heat transport through the membrane occurs by two mechanisms: heat transfer due to flux Q_N and heat transfer due to conduction Q_c, the latter considered as energy loss. The energy efficiency EE is defined as the ratio of the efficient heat due to flux and the total heat transported through the membrane Q_m and is calculated as:

$$Q_N = \Delta H * N \quad (6)$$

$$Q_c = \frac{k_m}{\delta}(T_{f,m} - T_{p,m}) \quad (7)$$

$$EE = \frac{Q_N}{Q_m} = \frac{Q_N}{Q_N + Q_c} \quad (8)$$

ΔH is the enthalpy of vaporization of water, $T_{f,m}$ and $T_{p,m}$ are the interfacial temperatures at the membrane on feed and permeate side and k_m is the thermal conductivity of the membrane, which is affected by the structure, porosity and intrinsic thermal conductivity of the polymer. These equations show that flux affects energy efficiency; hence all factors discussed in section 2.1 also have an impact on energy efficiency. Additionally, heat loss through the membrane can be reduced by tuning membrane parameters like thickness, porosity and thermal conductivity.

3 MATERIALS AND METHODS

3.1 Model structure

A MATLAB model is used to simulate the performance of the membranes. A schematic overview of the resistances is given in Figure 3.

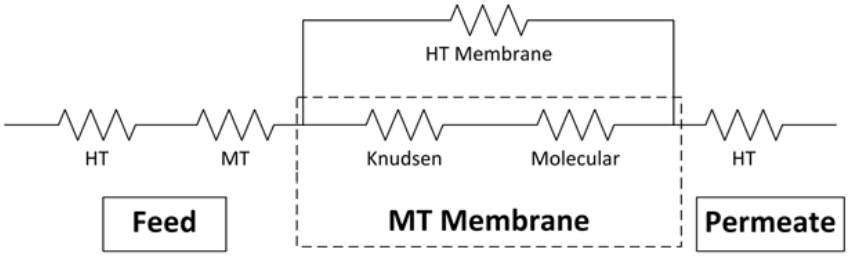

Figure 3: Schematic of the resistances in DCMD.

The mass transfer through the membrane is calculated using the Dusty Gas Model, which includes the Knudsen diffusion, molecular diffusion and viscous flow. In direct contact membrane distillation, viscous flow does not occur, because there is no total pressure difference across the membrane [1]. The relevant equations for the transitional flow between Knudsen and molecular diffusion in the Dusty Gas Model are given by Field et al., [11], where the degree of Knudsen transport in the transitional region is weighted based on the Knudsen number. The heat transfer through the membrane is calculated using equations 6 - 8. The heat transfer in the feed and permeate channels is calculated using a Nusselt type

equation obtained from the literature [39], which are further calibrated and validated by replacing the membrane with an aluminum foil [40]. The concentration polarization is incorporated in the model by using a Sherwood equation as a mass transfer equivalent for the Nusselt equations. The Generalized Likelihood Uncertainty Estimation (GLUE) method is used for a membrane based calibration [41]. The parameters which were used for calibration are the tortuosity and the thermal conductivity of the membrane matrix. Only in the case of the supported ePVDF membrane the Reynolds exponent in the Nusselt equation for the permeate channel was reduced by 13% in order to account for additional heat transfer resistance added by the non-woven support, as described by Hitsov et al. [42]. A set of commercially available membranes are experimentally investigated and simulated, for intensive calibration and validation of the model. More details on the build-up of the model and calibration are given by Hitsov et al. [42].

3.2 Membranes

In Table 2, an overview is given of the membranes used in this study. The ePVDF membrane is supported by an open non-woven fabric to provide mechanical strength; the other membranes are not supported.

Table 2: Properties of membranes as provided by manufacturers

Membrane Code	Provider	Trade name	Support layer	Polymer thermal conductivity
ePVDF	University of Liberec	Not commercial	Non-woven	0.19 [40]
PE	Pall	Supor-200R	No support	0.42-0.45 [43]
PVDF	Millipore	GVHP	No support	0.19 [40]
PP	Membrana	2E HF	No support	0.12 [40]

3.3 Porometry

The minimum, average and maximum pore diameter and pore size distribution were measured using a Porolux^{TM} 1000 device (Porometer, Eke, Belgium) as described by Francis et al. [44]. This instrument uses the wet/dry flow method. Porefil with a liquid surface tension of 16 mN/m was used as wetting liquid. The shape factor is assumed to be 1.

3.4 Liquid Entry Pressure

The liquid entry pressure (LEP) is the minimum pressure at which water wets the membrane

pores. The method to determine the LEP is described by Khayet *et al.* [45]. The pressure is increased stepwise with 0.1 bar each 30 seconds until a flow is detected. The pressure at which flow is detected is the LEP.

3.5 Pycnometry

The porosity of the membranes was determined by gas pycnometry [46]. A mold was used to cut the sample with fixed size. The volume of the membrane V_m was calculated by multiplying the area with the membrane thickness. The volume of the polymer matrix V_{po} was determined with a He-pycnometer (Micromeretics, Norcross, U.S.A). The supported membranes were delaminated and the support and the membrane were measured separately. The porosity was calculated as:

$$\epsilon = 1 - \frac{V_{po}}{V_m} \tag{9}$$

The average and deviation of 3 measurements are reported.

3.6 SEM

A cold field emission scanning electron microscope (SEM) type JSM6340F (JEOL, Tokyo, Japan) was used to study membrane cross-sections at an acceleration voltage of 5 keV. Cross-sections were obtained by a cross-section polisher type SM-09010 (JEOL, Tokyo, Japan) using an argon ion beam. All samples were coated with a thin Pt/Pd layer (~1.5 nm) using a Cressington HR208 high-resolution sputter-coater (Watford, England) to avoid charging by the e-beam. To obtain the thickness of the hydrophobic layer, the images of the cross-sections were analyzed in ImageJ. The average and deviation from 5 measurements are reported.

3.7 DCMD Setup

The membrane distillation performance was evaluated with a lab-scale DCMD setup (Figure 4). The flat-sheet module had an effective membrane surface of 0.0108 m^2. On the permeate side, purified water with electrical conductivity below 20 µS/cm was used. All tests were carried out using aqueous solutions with different salt concentrations ([NaCl] = 0, 150 and 300 g/kg). The feed and distillate were circulated counter-currently on their respective sides of the membrane using peristaltic pumps (Watson-Marlow, 520DuN/R2, Zwijnaarde, Belgium). The channel flow velocities were equal on the feed and permeate side and ranged

from 0.04 to 0.28 m/s. The temperature was kept constant using two heating baths (Huber, Ministat 230w-cc-NR, Offenburg, Germany) and monitored using four thermocouples (Thermo Electric Company, PT100 TF, Balen, Belgium). The average temperature (T_{av}) was kept constant at 52.5 °C for all experiments. The temperature difference (ΔT) over the membrane was varied between 6 °C and 20 °C. The flux was measured by evaluating the weight variations in the feed and distillate tank, using an analytical balance (Sartorius GmbH, ED8801-CW, Goettingen, Germany). The average of at least two experiments is reported. The electrical conductivity at the feed and permeate side were monitored by portable conductivity meters (WTW GmbH, pH/Cond 340i, Weilheim, Germany).

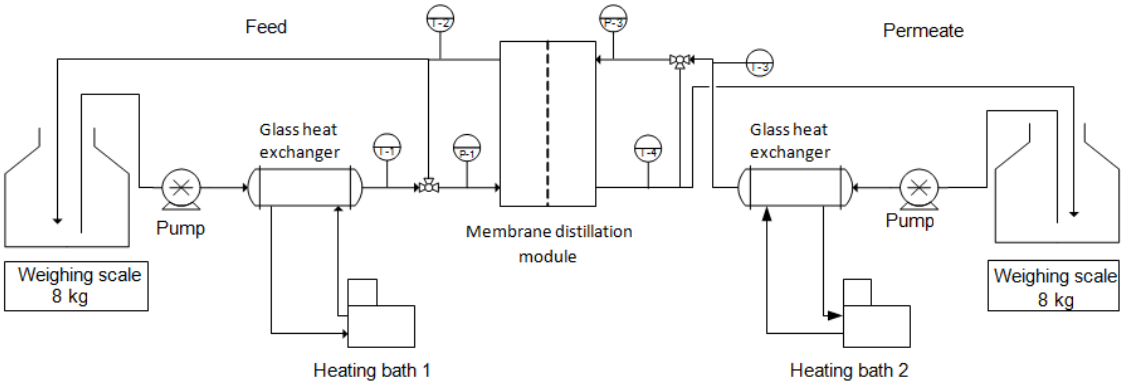

Figure 4: Schematic of the membrane distillation setup

The energy efficiency (EE) of the process is defined in equation 8. The total heat transfer through the membrane Q_m is considered to be equal to the heat transfer in the feed channel, as described by Khayet et al. [47].

$$EE\ (\%) = \frac{N\Delta HA}{FC_p\left(T_{f,in} - T_{f,out}\right)} \tag{10}$$

N is the water flux and ΔH the enthalpy of evaporation. F is the mass flow rate in the channels expressed in kg/s, A is the effective membrane surface area, C_p is the specific heat capacity of the feed solution, $T_{f,in}$ and $T_{f,out}$ are the bulk temperatures on feed side at the inlet and outlet of the module respectively. The same calculations were carried out for the permeate side and the average value and deviation is reported.

4 RESULTS & DISCUSSION

4.1 Membrane characterization

In order to evaluate and compare the membranes, the relevant properties that were

measured are summarized in Table 3. The thickness δ of the membranes ranges from 20 to 188 µm. The porosity ε varies in the order PP>ePVDF>PVDF>PE. The effect of pore size on flux is considered negligible in this study, because the range of the average pore diameter d_{av} of these membranes is relatively small (0.3-0.6 µm) and as stated by Ali et al., beyond a pore size of 0.3 µm the impact of pore size on flux is much less significant [12]. The calibrated tortuosity τ and membrane thermal conductivity k_m are obtained from the model. These calibrated values are close to the values reported in the literature for other comparable membranes [27], [48]. To provide mechanical strength, the ePVDF has a non-woven support with thickness 94 µm and porosity of 90%. The broader pore size distribution of this membrane results in a lower LEP.

Table 3: Measured and calculated properties of the membranes

Membrane	δ µm	ε %	d_{av} µm	LEP 10^5 Pa	Calibrated τ	Calibrated k_m W/(m.K)
ePVDF	20 ± 5	77% ± 3%	0.6	1.0	1.67	0.07
PE	95 ± 6	76% ± 3%	0.3	3.9	2.12	0.05
PVDF	112 ± 2	66% ± 3%	0.4	2.3	2.36	0.07
PP	188 ± 2	83% ± 2%	0.5	2.5	1.28	0.06

4.2 Salinity

To compare the DCMD performance of the different membranes considered in this study, flux and energy efficiency were measured at different salinities, ΔT = 6 °C, T_{av} = 52.5 °C and empty channel velocity v = 0.13 m/s. Additional information is obtained using simulations, which are indicated by the solid lines.

4.2.1 Flux

Figure 5 A shows the flux as a function of salt concentration. As discussed in section 2.1.2, the flux decreases with increasing salt concentration, because of the feed vapor pressure reduction due to the presence of salts (Eq. 3 and 4). Additionally, it is observed that the slope of the curves is less steep for thicker membranes, meaning that thicker membranes are less affected by salinity. This confirms the observations of Gostoli et al. that the flux of a thin membrane (60 µm) is more affected by salinity compared to a 1 cm thick membrane [18]. As stated in section 2.1.2, thinner membranes suffer more from temperature polarization and

therefore have a smaller ΔT_i under the same experimental conditions. Since the effect of salinity on the driving force is more pronounced at smaller ΔT_i (Figure 2), the flux of thinner membranes is more affected by salinity.

For pure water, the thinnest membrane (ePVDF) shows the highest flux. The flux of the thickest membrane (PP) is higher compared to the flux of the PVDF and PE membrane. This indicates that for pure water, other membrane parameters beside thickness also play an important role. In this case, the higher porosity and lower tortuosity of the PP membrane compared to the PVDF and PE membrane positively affects the flux (Table 3).

At higher salt concentrations, negative fluxes are observed. This negative flux is caused by the reverse osmotic driving force due to the presence of salts at the feed side (section 2.1.2). For a fixed bulk driving force, thicker membranes exhibit positive fluxes up to higher concentrations, because the temperature polarization is much more pronounced for thinner membranes (section 2.1.1) and a thicker membrane is able to sustain a higher interfacial temperature difference (ΔT_i). For example, at 250 g/kg, the minimum ΔT_i needed to achieve a positive vapor pressure difference over the membrane is not achieved for the ePVDF (20 µm), resulting in negative flux of -5 kg/m^2.h. The thicker PVDF (112 µm) and PP (188 µm) and PE (95 µm) membranes show positive fluxes at 250 g/kg under these experimental conditions, because the ΔT_i is still sufficient to sustain a positive vapor pressure difference over the membrane.

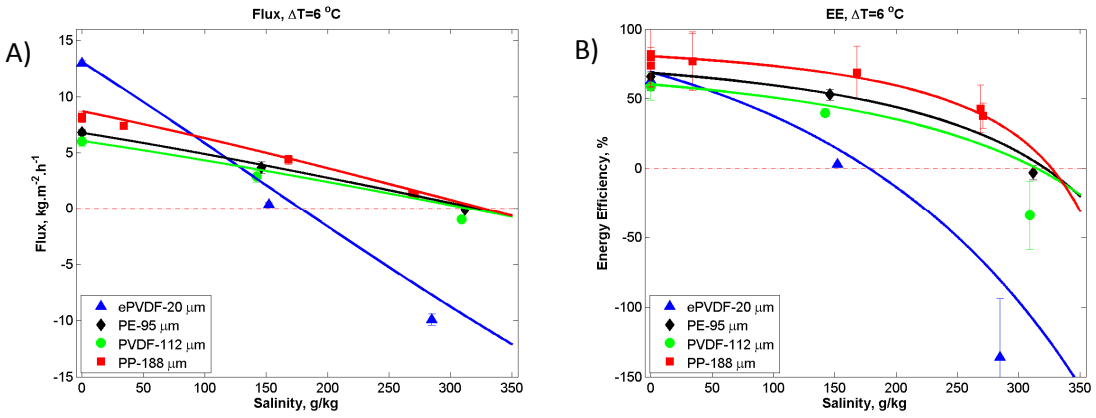

Figure 5: Flux (A) and energy efficiency (B) as a function of salinity for membranes with different thicknesses. Markers: experimental, lines: model predictions

4.2.2 Energy efficiency

Figure 5 B shows decreasing energy efficiency with increasing salt concentration. While the

flux is reduced with increasing salt concentration (Figure 5 A), the driving force for the heat loss due to conduction is not affected by this phenomenon (eq. 6 - 8). The highest energy efficiencies for pure water were observed for the more porous membranes, while the membrane thickness seems to have little effect on energy efficiency under these conditions. At higher salinities the conclusions are comparable to the observations for the flux: the energy efficiency of thicker membranes is less affected by salinity, while a severe drop of the energy efficiency is observed for thin membranes. Note that the deviation of the experimental values are relatively large at higher salinities, because the temperature drop in the feed channel (± 1 °C) approaches the temperature sensor error (± 0.2 °C).

4.3 Temperature and flow velocity

As discussed in previous section, the choice of the membrane depends on salinity. In this section, the effects of process conditions are investigated for the thinnest and the thickest membrane, namely PP and ePVDF, for the whole solubility range of NaCl. The effect of bulk temperature difference over the membrane is studied in the range from 6° to 20°C. Higher temperature differences are out of the scope of this article, because this is not realistic for full scale DCMD. The effects of flow velocity are tested in the range of 0.04 to 0.28 m/s. For large scale DCMD, flow velocity is limited, because the pressure drop increases with increasing flow velocity [24], [49].

4.3.1 Flux

Figure 6 shows the flux as function of salinity for the thick PP and thin ePVDF membrane at different ΔT_b and flow velocities. As already described in literature, the flux improves upon increasing ΔT_b and flow velocities for all concentrations tested [26], [51]. Moreover, the effect is more pronounced for the thin ePVDF membranes. While the thick PP membrane achieves positive fluxes for all tested concentrations, negative fluxes are observed for the thin ePVDF membrane when low flow velocities or temperature differences are applied. Moreover, to achieve comparable fluxes, higher temperature differences or flow velocities are needed for the ePVDF membrane. This indicates that the ePVDF loses much more of the driving force due to temperature polarization, enlarging the negative effect of salinity (see also section 4.2.1). When increasing the flow velocity from 0.04 m/s up to 0.28 m/s, flux for pure water improves with a factor 1.6 for the PP membrane and a factor 2.5 for the ePVDF membrane. Also note the PP membrane approaches the region where flow velocity does not

further improves the flux at flow velocity 0.28 cm/s [20], [34]. Yet, the flux of the thin ePVDF is enhanced at flow velocity 0.28 cm/s. The membrane resistance of the PP is larger compared to ePVDF, hence the temperature polarization is less pronounced for this membrane. Additionally, the resistance of the fluid is relatively smaller compared to the resistance in the membrane, meaning that the PP membrane is limited by membrane resistance, while the ePVDF is limited by hydrodynamics.

In general, by increasing ΔT_b or flow velocity, the driving force for flux is increased and the fluxes are improved at all tested salt concentrations. The effects are larger for thin membranes, indicating that thin membranes are more sensitive to process conditions, while the thicker membranes are more limited by membrane resistance.

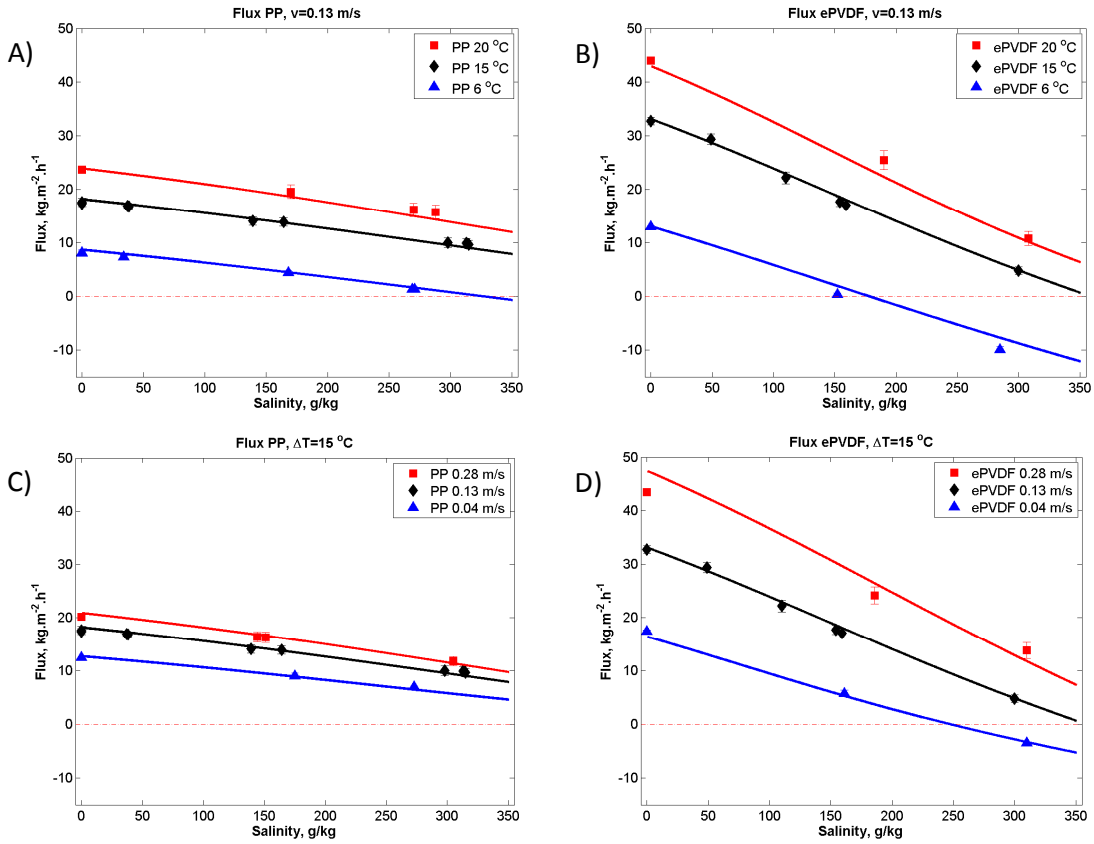

Figure 6: Effect of temperature difference (A and B) and flow velocity (C and D) on flux for the PP (A and C) and the ePVDF membrane (B and D)

4.3.2 Energy efficiency

Comparable to flux, energy efficiency reduces at higher salinities. According to Figure 7, the effect is larger for the ePVDF membrane, especially at low flow velocities or low temperature

difference. The PP membrane also shows a large decline at low temperature difference over the membrane, but this effect is smaller compared to the thinner ePVDF membrane under the same conditions. The reduced energy efficiency at high salinities is caused by the reduced flux at high salinity (Eq. 3 – 5), while the heat transfer due to conduction is not directly affected by salinity (Eq. 7). Therefore, energy efficiency reduces more in the cases where flux reduction is larger, particularly for the thin ePVDF membranes, at lower bulk temperature differences and at low flow velocities (Figure 7). In section 4.3.1, it was already discussed that higher driving force is needed for the ePVDF membrane to achieve the same flux as the PP membrane at 300 g/kg. This means also more energy input to achieve the same fluxes and hence a lower energy efficiency. This can also be observed in Figure 7. While for the PP energy efficiencies around 60-70% are achieved at high salinities, the maximum energy efficiency at high salinity is 31% for the ePVDF membrane.

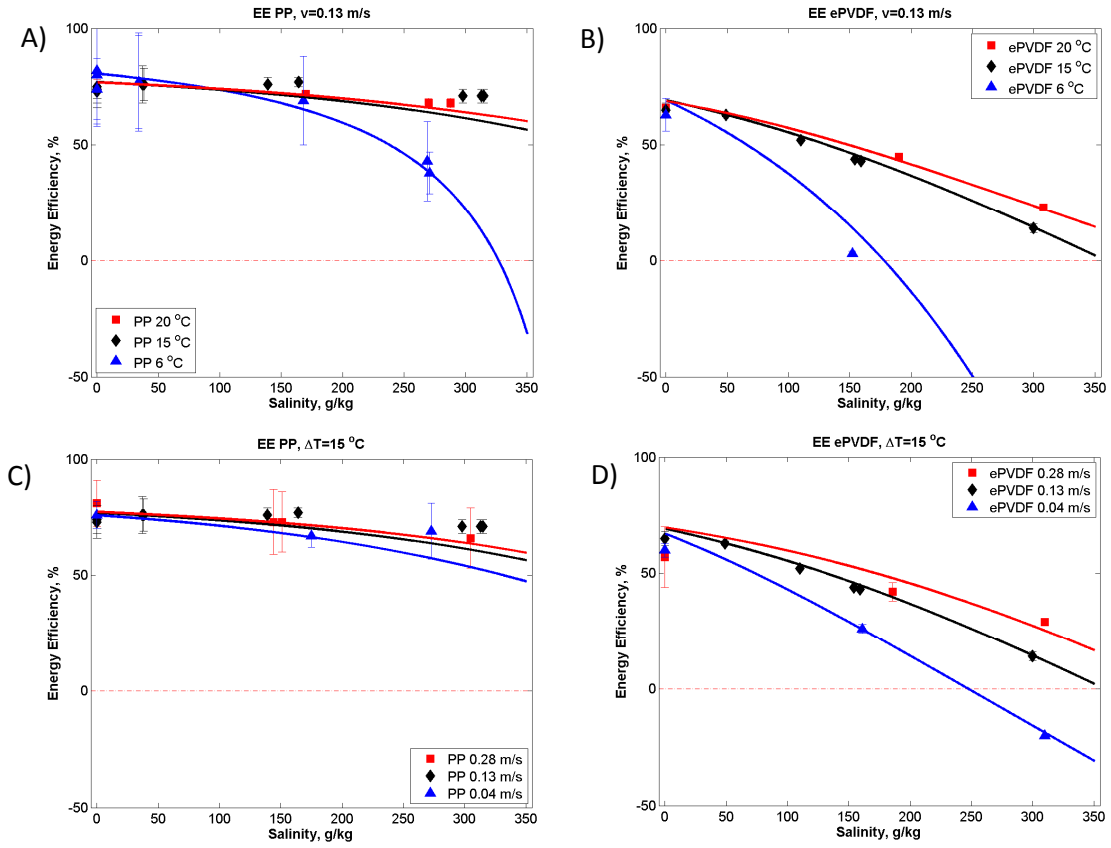

Figure 7: Effect of temperature difference (A and B) and flow velocity (C and D) on energy efficiency for the PP (A and C) and the ePVDF membrane (B and D)

4.4 Optimal thickness

Previous sections indicated the importance of the membrane thickness. For low salinities,

thin membranes seem to be more interesting, which is also confirmed in the literature [19], [21]. On the contrary, thicker membranes perform better at higher salinities. To investigate this in more detail, the flux and energy efficiency was modelled as a function of membrane thickness (1 – 250 µm) at different salinities and fixed process conditions in Figure 8. The parameters and the calibration set of the PP membrane are used, hereby excluding the influence of other structural parameters while varying the PP membrane thickness. It should be noted that these results are an extrapolation from the calibrated thickness for a thicker or a thinner membrane. To justify this, the model is thoroughly calibrated and validated [42].

Upon decreasing the membrane thickness, both mass and heat transfer through the membrane are improved. For pure water and decreasing membrane thickness, the effect of increasing permeability (section 2.1.1) is more important compared to the reduction of the driving force due to the increased temperature polarization (Eq. 7). Accordingly, thinner membranes show higher fluxes. For saline water, Figure 8 A supports the existence of an optimal membrane thickness for flux indicated by the markers [19]–[21]. The vapor pressure is additionally reduced by the presence of salts. As discussed in 4.2.1, with decreasing membrane thickness the effect of salinity becomes more pronounced. At a certain thickness, the reduction of the driving force due to temperature polarization and salts counterbalances the increased permeability, resulting in an optimum membrane thickness for flux, depending on concentration; as thin as physically possible for clean water and from 6 µm at 30 g/kg up to 49 µm at 320 g/kg under these experimental conditions. Further decrease of the membrane thickness beyond the optimum leads to negative (osmotic) fluxes. It can be concluded that depending on salinity, an optimal membrane thickness exists and thicker membranes are needed at higher salinity.

The effect of thickness on the energy efficiency is shown in Figure 8 B. For pure water, the energy efficiency is not affected by membrane thickness: because both heat due to conduction and mass transfer are equally promoted, their ratio remains the same (Eq. 8). In salty water, the energy efficiency is relatively unaffected by the membrane thickness in the thicker membrane range. At low membrane thickness, the sharp decline of the flux results in a severe drop in energy efficiency. These observations are consistent with the literature [19].

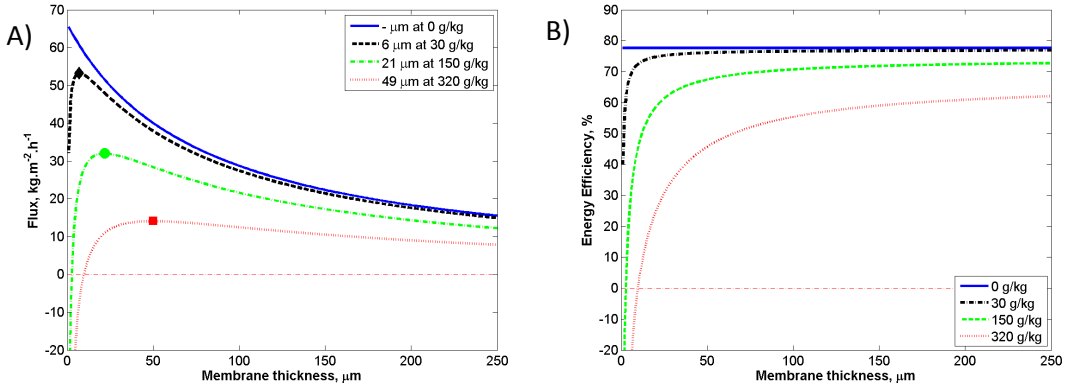

Figure 8: Flux (A) and energy efficiency (B) as function of membrane thickness for different salinities. PP, T_{av} = 52.5 °C, ΔT = 15 °C, v = 0.13 m/s

4.4.1 Membrane structure

As discussed in section 2.1 and visualized in Figure 1, the membrane structure affects flux, energy efficiency and the temperature polarization phenomena. In this section, the effect of the membrane parameters is investigated by simulating the flux and energy efficiency as function of membrane thickness. The effect of tortuosity is investigated by plotting flux and energy efficiency as function of thickness for the PP calibration set with the calibrated value for tortuosity 1.28 and a hypothetical tortuosity of 2.56 for the same calibration set. The same is done for porosity (hypothetical value 60%, the measured value 83%, hypothetical value 93%) and thermal conductivity (the calibrated value 0.06 W/m.K and hypothetical value 0.12 W/m.K) in Figure 9. The same membrane parameters, calibration set and experimental conditions are used as in section 4.3. The salt concentration equals 150 g/kg for all figures.

A lower tortuosity and higher porosity both increase the membrane permeability and higher flux for all membrane thicknesses (Figure 9 A and C). Additionally, a higher porosity and a lower thermal conductivity reduce the heat loss through the membrane. The higher interfacial temperature difference over the membrane results in higher fluxes for all membrane thicknesses (Figure 9 C and E). Energy efficiency is improved for lower tortuosity, higher porosity and lower membrane thermal conductivity. In these cases, the flux is improved, while heat loss due to conduction is not affected (tortuosity) or even reduced (porosity and thermal conductivity). The optimal thickness indicated by the marker reduces for the cases where the temperature polarization is reduced. For higher tortuosity, the lower

fluxes reduce the temperature polarization, while a reduced thermal conductivity of the membrane reduces the heat transfer due to conduction. The porosity has a small effect on the optimal thickness of the membrane, because the improved flux and reduced thermal conductivity of more porous membranes are counteracting in terms of temperature polarization.

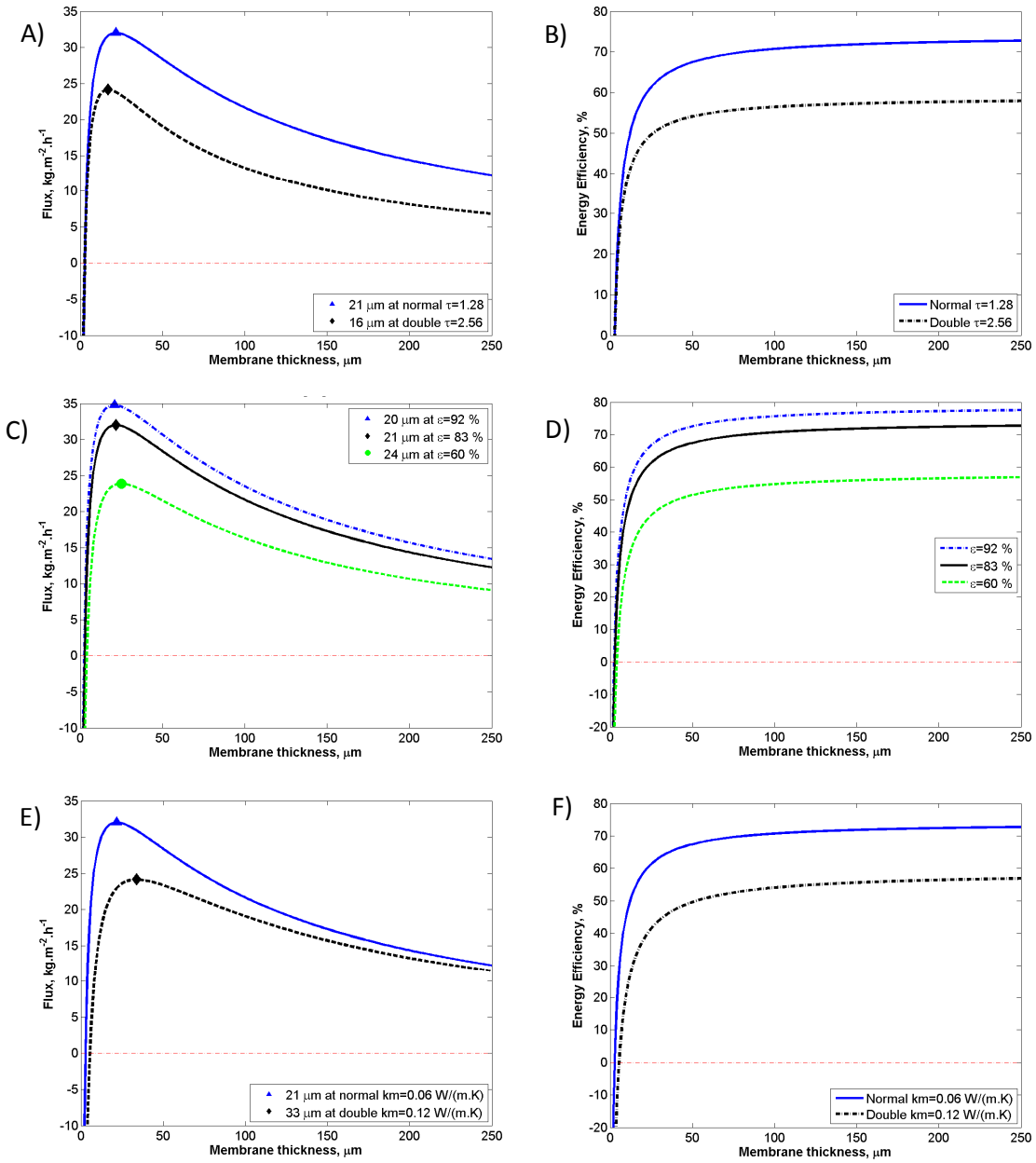

Figure 9: Flux (A, C, E) and energy efficiency (B, D, F) as function of membrane thickness for different porosities (A, B), tortuosity (C, D) and membrane thermal conductivity (E, F). PP, T_{av} = 52.5 °C, ΔT = 15 °C, v = 0.13 m/s, [NaCl]= 150 g/kg

4.4.2 Temperature and flow velocity

The effect of process conditions on the flux and optimal thickness at salt concentration of 150 g/kg is shown in Figure 10 A and C. When increasing the temperature difference and flow velocity, the flux increases. In contrast, the optimal thickness for flux decreases. Due to the more pronounced temperature polarization, thinner membranes need a higher bulk driving force or flow velocity to be able to sustain a sufficiently high interfacial temperature difference over the membrane. This indicates that the choice of membrane thickness depends on the experimental conditions. Figure 10 B and D indicate that a large temperature difference and high flow velocity are important to achieve high energy efficiency, especially for thin membranes.

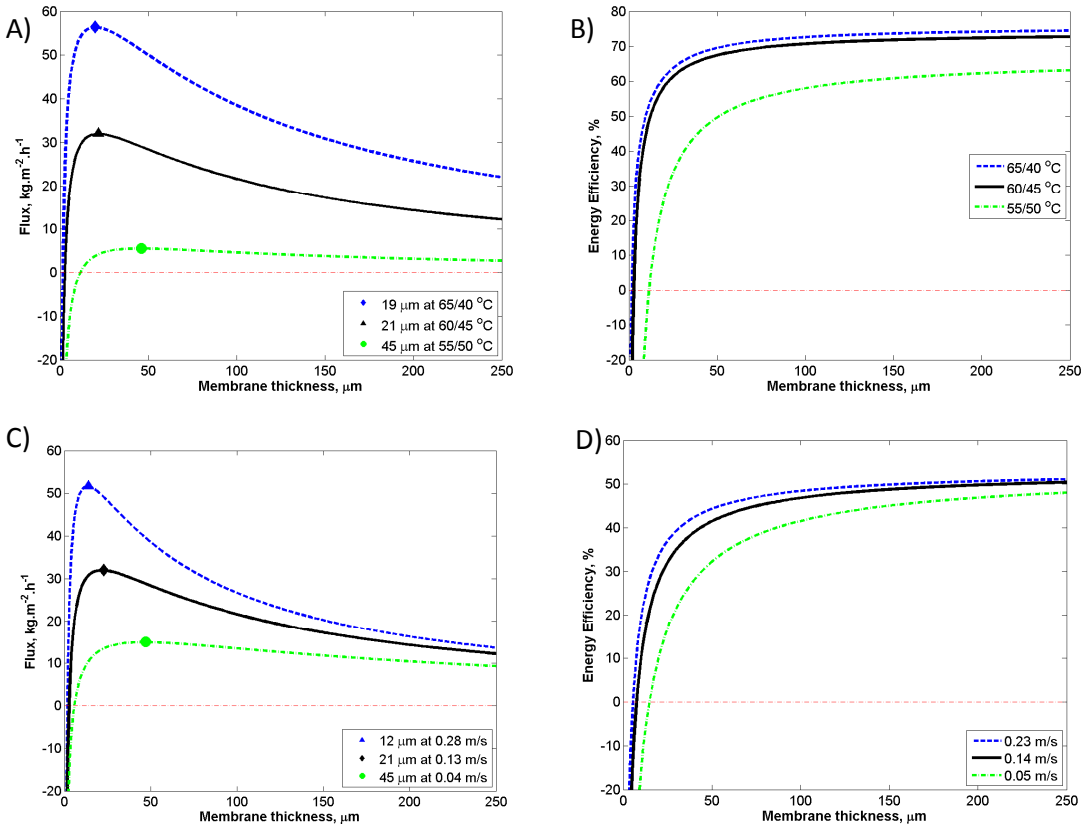

Figure 10: Water flux (A and C) and energy efficiency (B and D) as function of membrane thickness at different ΔT (A and B) and flow velocities (C and D).
PP, v = 0.13 m/s, ΔT = 15 °C, [NaCl] = 150 g/kg

Since the optimal membrane thickness depends on the membrane characteristics as well as the process conditions it is impossible to give a straightforward recommendation on what membrane thickness should be used under which conditions. However, as a guideline Table 4

is given, where the range of the optimal thickness is given for the studied membranes at different operational conditions, together with the corresponding flux and energy efficiency. It should be used only as a guideline for the possible range of membrane thickness and the kind of fluxes and energy efficiencies, which are possible at the given conditions and for a variety of membrane structures.

Table 4: Minimum and maximum optimal thickness and corresponding flux and energy efficiency computed for the 4 membranes in different conditions.

Driving force

Temperature		**60-54 °C**		**60-40 °C**	
Flow velocity		**0.04 m/s**	**0.28 m/s**	**0.04 m/s**	**0.28 m/s**
30 g/l	**δ, µm**	15 - 30	4 - 9	8 - 15	2 - 4
	N, kg/(h.m^2)	7 - 9	21 - 34	22 - 32	70 - 110
	EE, %	51 - 71	50 - 70	48 - 69	46 - 68
150 g/l	**δ, µm**	58 - 112	16 - 35	25 - 47	7 - 14
	N, kg/(h.m^2)	2 - 4	8 - 14	13 - 20	44 - 68
	EE, %	35 - 55	34 - 54	39 - 59	37 - 58
320 g/l	**δ, µm**	414 - 793	120 - 252	57 - 102	16 - 31
	N, kg/(h.m^2)	0.1 - 0.2	0.3 - 0.8	6 - 10	21 - 33
	EE, %	9 - 20	9 - 20	29 - 47	28 - 46

Flux ↑ / Optimal thickness ↓ (Flux/Energy efficiency)

Flux

Optimal thickness

5 CONCLUSIONS

In this paper, it is shown that the salinity of the feed is an important factor to take into account when designing a DCMD system. Since salinity reduces the feed vapor pressure by a fixed percentage, the most important factor determining the effect of salinity on the performance is the interfacial temperature difference over the membrane. Additionally, the selection of the membrane is found to be critical for optimizing the membrane distillation process. For pure water, thinner membranes show higher fluxes. With increasing salinity, both flux and energy efficiency of thin membranes are severely reduced, especially at low temperature differences and flow velocities. Therefore, at high salinities, thin membranes can only be used if sufficient driving force is provided. In these cases, a thicker membrane should be preferably used, because of the much higher energy efficiency. At higher salinities, an optimal membrane thickness exists, which is decreasing for higher tortuosity, lower membrane thermal conductivity, higher porosity, lower salt concentration, higher bulk temperature difference and higher flow velocity. The optimal membrane thickness computed

in this article ranges from 2 - 739 µm for concentrations of NaCl ranging from 30 up 320 g/l.

6 ACKNOWLEDGEMENTS

The authors want to express their thanks to the VITO personnel for their continuous support, especially T. Van Mechelen, J. Boeckx, A. Claes, L. Stoops and M. Dubreuil (Unit Separation & Conversion Technology, VITO). L. Eykens and I. Hitsov thankfully acknowledges a PhD scholarship provided by VITO. Additionally, the authors would like to thank Tomas Jiricek and Tomas Lederer from the Technical University of Liberec (Czech Republic) for providing the ePVDF membrane and Bart Nelemans from Aquastill for providing the PE membrane.

7 BIBLIOGRAPHY

[1] K. W. Lawson and D. R. Lloyd, "Membrane distillation. II. Direct contact MD," *J. Memb. Sci.*, vol. 120, no. 1, pp. 123–133, Oct. 1996.

[2] N. Ghaffour, T. M. Missimer, and G. L. Amy, "Technical review and evaluation of the economics of water desalination: Current and future challenges for better water supply sustainability," *Desalination*, vol. 309, pp. 197–207, Jan. 2013.

[3] J. Ku and S. Lee, "Comparison of Direct Contact Membrane Distillation , Vacuum Membrane Distillation and Air Gap Membrane Distillation for RO Brine Treatment Seawater Desalination," no. 6.

[4] M. S. El-Bourawi, Z. Ding, R. Ma, and M. Khayet, "A framework for better understanding membrane distillation separation process," *J. Memb. Sci.*, vol. 285, no. 1–2, pp. 4–29, Nov. 2006.

[5] F. Edwie and T. Chung, "Development of simultaneous membrane distillation – crystallization (SMDC) technology for treatment of saturated brine," *Chem. Eng. Sci.*, vol. 98, pp. 160–172, 2013.

[6] X. Ji, E. Curcio, S. Al Obaidani, G. Di Profio, E. Fontananova, and E. Drioli, "Membrane distillation-crystallization of seawater reverse osmosis brines," *Sep. Purif. Technol.*, vol. 71, no. 1, pp. 76–82, Jan. 2010.

[7] R. Creusen, J. van Medevoort, M. Roelands, A. van Renesse van Duivenbode, J. H. Hanemaaijer, and R. van Leerdam, "Integrated membrane distillation–crystallization: Process design and cost estimations for seawater treatment and fluxes of single salt solutions," *Desalination*, pp. 2–10, Mar. 2013.

[8] F. He, J. Gilron, H. Lee, L. Song, and K. K. Sirkar, "Potential for scaling by sparingly soluble salts in crossflow DCMD," *J. Memb. Sci.*, vol. 311, no. 1–2, pp. 68–80, Mar. 2008.

[9] C. Mya, A. Gordon, J. Thomas, and R. Sheikholeslami, “Membrane distillation crystallization of concentrated salts — flux and crystal formation,” *J. Memb. Sci.*, vol. 257, pp. 144–155, 2005.

[10] E. Curcio, X. Ji, G. Di Profio, A. O. Sulaiman, E. Fontananova, and E. Drioli, “Membrane distillation operated at high seawater concentration factors: Role of the membrane on CaCO3 scaling in presence of humic acid,” *J. Memb. Sci.*, vol. 346, no. 2, pp. 263–269, Jan. 2010.

[11] R. W. Field, H. Y. Wu, and J. J. Wu, “Multiscale Modeling of Membrane Distillation: Some Theoretical Considerations,” *Ind. Eng. Chem. Res.*, vol. 52, no. 26, pp. 8822–8828, Jul. 2013.

[12] M. I. Ali, E. K. Summers, H. a. Arafat, and J. H. L. V, “Effects of membrane properties on water production cost in small scale membrane distillation systems,” *Desalination*, vol. 306, pp. 60–71, Nov. 2012.

[13] S. Adnan, M. Hoang, H. Wang, and Z. Xie, “Commercial PTFE membranes for membrane distillation application: Effect of microstructure and support material,” *Desalination*, vol. 284, pp. 297–308, Jan. 2012.

[14] J. Zhang, N. Dow, M. Duke, E. Ostarcevic, J.-D. Li, and S. Gray, “Identification of material and physical features of membrane distillation membranes for high performance desalination,” *J. Memb. Sci.*, vol. 349, no. 1–2, pp. 295–303, Mar. 2010.

[15] G. Rao, S. R. Hiibel, and A. E. Childress, “Simplified flux prediction in direct-contact membrane distillation using a membrane structural parameter,” *Desalination*, vol. 351, pp. 151–162, Oct. 2014.

[16] S. Bonyadi and T. S. Chung, “Flux enhancement in membrane distillation by fabrication of dual layer hydrophilic–hydrophobic hollow fiber membranes,” *J. Memb. Sci.*, vol. 306, no. 1–2, pp. 134–146, Dec. 2007.

[17] M. Essalhi and M. Khayet, “Self-sustained webs of polyvinylidene fluoride electrospun nanofibers at different electrospinning times: 1. Desalination by direct contact membrane distillation,” *J. Memb. Sci.*, vol. 433, pp. 167–179, Jan. 2013.

[18] C. Gostoli, G. C. Sarti, and S. Matulli, “Low Temperature Distillation Through Hydrophobic Membranes,” *Sep. Sci. Technol.*, vol. 22, no. 2, pp. 855–872, 1987.

[19] L. Martínez and J. M. Rodríguez-Maroto, “Membrane thickness reduction effects on direct contact membrane distillation performance,” *J. Memb. Sci.*, vol. 312, no. 1–2, pp. 143–156, Apr. 2008.

[20] F. Laganà, G. Barbieri, and E. Drioli, “Direct contact membrane distillation: modelling and concentration experiments,” *J. Memb. Sci.*, vol. 166, no. 1, pp. 1–11, Feb. 2000.

[21] H. Y. Wu, R. Wang, and R. W. Field, “Direct contact membrane distillation: An experimental and analytical investigation of the effect of membrane thickness upon transmembrane flux,” *J. Memb. Sci.*, vol. 470, pp. 257–265, Nov. 2014.

[22] M. Essalhi and M. Khayet, “Self-sustained webs of polyvinylidene fluoride electrospun nanofibers at different electrospinning times: 2. Theoretical analysis, polarization effects and thermal efficiency,” *J. Memb. Sci.*, vol. 433, pp. 167–179, Jan. 2013.

[23] E. Drioli, A. Ali, and F. Macedonio, “Membrane distillation: Recent developments and perspectives,” *Desalination*, Oct. 2014.

[24] D. Winter, J. Koschikowski, and M. Wieghaus, “Desalination using membrane distillation: Experimental studies on full scale spiral wound modules,” *J. Memb. Sci.*, vol. 375, no. 1–2, pp. 104–112, Jun. 2011.

[25] Y. Yun, R. Ma, W. Zhang, A. G. Fane, and J. Li, “Direct contact membrane distillation mechanism for high concentration NaCl solutions,” *Desalination*, vol. 188, no. February 2005, pp. 251–262, 2006.

[26] Y. Guan, J. Li, F. Cheng, J. Zhao, and X. Wang, “Influence of salt concentration on DCMD performance for treatment of highly concentrated NaCl, KCl, MgCl2 and MgSO4 solutions,” *Desalination*, vol. 355, pp. 110–117, Jan. 2015.

[27] M. Khayet and T. Matsuura, *Membrane distillation: principles and applications*. Elsevier B.V., 2011.

[28] M. Khayet, “Membranes and theoretical modeling of membrane distillation: a review.,” *Adv. Colloid Interface Sci.*, vol. 164, no. 1–2, pp. 56–88, May 2011.

[29] J. Phattaranawik, R. Jiraratananon, and A. G. Fane, “Effect of pore size distribution and air flux on mass transport,” *J. Memb. Sci.*, vol. 215, pp. 75–85, 2003.

[30] C. Cabassud and D. Wirth, “Membrane distillation for water desalination: How to chose an appropriate membrane?,” *Desalination*, vol. 157, no. 1–3, pp. 307–314, Aug. 2003.

[31] K. W. Lawson, M. S. Hall, and D. R. Lloyd, “Compaction of microporous membranes used in membrane distillation. I. Effect on gas permeability,” *J. Memb. Sci.*, vol. 101, no. 1–2, pp. 99–108, May 1995.

[32] M. Qtaishat, T. Matsuura, B. Kruczek, and M. Khayet, “Heat and mass transfer analysis in direct contact membrane distillation,” *Desalination*, vol. 219, no. 1–3, pp. 272–292, Jan. 2008.

[33] A. O. Imdakm and T. Matsuura, “Simulation of heat and mass transfer in direct contact membrane distillation (MD): The effect of membrane physical properties,” *J. Memb. Sci.*, vol. 262, pp. 117–128, 2005.

[34] A. Bahmanyar, M. Asghari, and N. Khoobi, “Numerical simulation and theoretical study on simultaneously effects of operating parameters in direct contact membrane distillation,” *Chem. Eng. Process. Process Intensif.*, vol. 61, pp. 42–50, Nov. 2012.

[35] L. Martinez-Diez and M. I. Vazques-Gonzalez, “Temperature and concentration polarization in membrane distillation of aqueous salt solutions,” *J. Memb. Sci.*, vol. 156, pp. 265–273, 1999.

[36] T. Y. Cath, V. D. Adams, and A. E. Childress, “Experimental study of desalination using direct contact membrane distillation: a new approach to flux enhancement,” *J. Memb. Sci.*, vol. 228, no. 1, pp. 5–16, Jan. 2004.

[37] I. Hitsov, T. Maere, K. De Sitter, C. Dotremont, and I. Nopens, “Modelling approaches in Membrane Distillation : A critical review,” *Sep. Purif. Technol.*, 2014.

[38] M. Gryta, “Osmotic MD and other membrane distillation variants,” *J. Memb. Sci.*, vol. 246, no. 2, pp. 145–156, Jan. 2005.

[39] M. Gryta, M. Tomaszewska, and a. W. Morawski, “Membrane distillation with laminar flow,” *Sep. Purif. Technol.*, vol. 11, no. 2, pp. 93–101, Jun. 1997.

[40] J. Phattaranawik, R. Jiraratananon, and a. . Fane, “Heat transport and membrane distillation coefficients in direct contact membrane distillation,” *J. Memb. Sci.*, vol. 212, no. 1–2, pp. 177–193, Feb. 2003.

[41] K. Beven and A. Binley, “The future of distributed models: Model calibration and uncertainty prediction,” *Hydrol. Process.*, vol. 6, pp. 276–298, 1992.

[42] I. Hitsov, L. Eykens, K. De Sitter, C. Dotremont, and I. Nopens, “Calibration And Analysis Of A Direct Contact Membrane Distillation Model Using The GLUE Method,” *Manustript Prep.*, 2015.

[43] T. Osswald and J. P. Hernández-Ortiz, *Polymer processing.* Munich: Hanser Publishers, 2006.

[44] L. Francis, N. Ghaffour, a. S. Alsaadi, S. P. Nunes, and G. L. Amy, “Performance evaluation of the DCMD desalination process under bench scale and large scale module operating conditions,” *J. Memb. Sci.*, vol. 455, pp. 103–112, Apr. 2014.

[45] M. Khayet and T. Matsuura, “Preparation and Characterization of Polyvinylidene Fluoride Membranes for Membrane Distillation,” *Ind. Eng. Chem. Res.*, vol. 40, pp. 5710–5718, 2001.

[46] S. S. Sreedhara and N. R. Tata, “A Novel Method for Measurement of Porosity in Nanofiber Mat using Pycnometer in Filtration,” vol. 8, no. 4, pp. 132–137, 2013.

[47] M. Khayet, “Solar desalination by membrane distillation: Dispersion in energy consumption analysis and water production costs (a review),” *Desalination*, vol. 308, pp. 89–101, Jan. 2013.

[48] M. C. García-Payo and M. a Izquierdo-Gil, “Thermal resistance technique for measuring the thermal conductivity of thin microporous membranes,” *J. Phys. D. Appl. Phys.*, vol. 37, no. 21, pp. 3008–3016, Nov. 2004.

[49] A. E. Jansen, J. W. Assink, J. H. Hanemaaijer, J. Van Medevoort, and E. Van Sonsbeek, “Development and pilot testing of full-scale membrane distillation modules for deployment of waste heat,” *Desalination*, vol. 323, pp. 55–65, 2013.

[50] V. a. Bui, L. T. T. Vu, and M. H. Nguyen, “Simulation and optimisation of direct contact membrane distillation for energy efficiency,” *Desalination*, vol. 259, no. 1–3, pp. 29–37, Sep. 2010.

[51] D. Winter, J. Koschikowski, D. Düver, P. Hertel, and U. Beuscher, “Evaluation of MD process performance : Effect of backing structures and membrane properties under different operating conditions,” *DES*, vol. 323, pp. 120–133, 2013.